Title

cAMP-dependent activation of the Rac guanine exchange factor P-REX1 by type I protein kinase A (PKA) regulatory subunits.

Journal

Journal of Biological Chemistry, 294(7)

Authors

Adame-García, Sendi

Cervantes-Villagrana, Rodolfo

Orduña-Castillo, Lennis

et al.

Publication Date

2019-02-15

DOI

10.1074/jbc.RA118.006691

Peer reviewed

cAMP-dependent activation of the Rac guanine exchange factor P-REX1 by type I protein kinase A (PKA) regulatory subunits

Received for publication, November 13, 2018, and in revised form, November 29, 2018 Published, Papers in Press, December 10, 2018, DOI 10.1074/jbc.RA118.006691

Sendi Rafael Adame-García[‡1], Rodolfo Daniel Cervantes-Villagrana[§1], Lennis Beatriz Orduña-Castillo[‡1], Jason C. del Rio[¶], J. Silvio Gutkind[¶‖2], Guadalupe Reyes-Cruz[‡], Susan S. Taylor[¶‡‡], and José Vázquez-Prado[§3]**

*From the Departments of [‡]Cell Biology and [§]Pharmacology, Center for Research and Advanced Studies of the National Polytechnic Institute (CINVESTAV-IPN), 07360 Mexico City, Mexico and [‖]Moores Cancer Center and the Departments of [¶]Pharmacology, **Chemistry and [‡‡]Biochemistry, University of California San Diego, La Jolla, California 92093*

Edited by Roger J. Colbran

Regulatory subunits of protein kinase A (PKA) inhibit its kinase subunits. Intriguingly, their potential as cAMP-dependent signal transducers remains uncharacterized. We recently reported that type I PKA regulatory subunits (RIα) interact with phosphatidylinositol 3,4,5-trisphosphate–dependent Rac exchange factor 1 (P-REX1), a chemotactic Rac guanine exchange factor (RacGEF). Because P-REX1 is known to be phosphorylated and inhibited by PKA, its interaction with RIα suggests that PKA regulatory and catalytic subunits may fine-tune P-REX1 activity or those of its target pools. Here, we tested whether RIα acts as a cAMP-dependent factor promoting P-REX1–mediated Rac activation and cell migration. We observed that G_s-coupled EP2 receptors indeed promote endothelial cell migration via RIα-activated P-REX1. Expression of the P-REX1–PDZ1 domain prevented RIα/P–REX1 interaction, P-REX1 activation, and EP2-dependent cell migration, and P-REX1 silencing abrogated RIα-dependent Rac activation. RIα-specific cAMP analogs activated P-REX1, but lost this activity in RIα-knockdown cells, and cAMP pulldown assays revealed that P-REX1 preferentially interacts with free RIα. Moreover, purified RIα directly activated P-REX1 *in vitro*. We also found that the RIα CNB-B domain is critical for the interaction with P-REX1, which was increased in RIα mutants, such as the acrodysostosis-associated mutant, that activate P-REX1 at basal cAMP levels. RIα and Cα PKA subunits targeted distinct P-REX1 molecules, indicated by an absence of phosphorylation in the active fraction of P-REX1. This was in contrast to the inactive fraction in which phosphorylated P-REX1 was present, suggesting co-existence of dual stimulatory and inhibitory effects. We conclude that PKA's regulatory subunits are cAMP-dependent signal transducers.

The widely recognized role of cAMP as a second messenger controlling fundamental cellular processes, such as cell growth, adhesion, and polarized migration, has mainly been attributed to phosphorylation-dependent effects of the catalytic (C)[4] subunits of cAMP-dependent protein kinase A (PKA) (1). The dimeric regulatory (R) subunits, containing two cAMP-binding domains in each monomer as well as a docking and dimerization domain, restrict the subcellular localization of the tetrameric holoenzyme, keeping the two C-subunits inhibited in the absence of cAMP. In response to increasing concentrations of cAMP, this second messenger is captured by the cAMP-binding domains, causing conformational changes that reduce the affinity of R-subunits for the C-subunits, thereby unleashing their catalytic activity and enabling them to phosphorylate diverse effectors that control a plethora of biological pathways (2).

PKA has served as prototype to understand the structural characteristics of the whole-human kinome (3). Remarkably, its multimeric organization, with independent regulatory cAMP-sensing domains as part of dissociable regulatory subunits (RIα, RIβ, RIIα, and RIIβ), is a unique feature among kinases (2). Studies on the regulatory subunits have focused on their role in controlling their kinase partners. By interacting with A kinase-anchoring proteins (AKAPs), the PKA R-subunits also localize PKA holoenzyme pools to precise subcellular compartments facilitating the phosphorylation of specific substrates, fre-

This work was supported in part by CONACyT (Consejo Nacional de Ciencia y Tecnología, Mexico) Grants 286274 (to J. V.-P.) and 240119 (to G. R.-C.) and National Institutes of Health Grant R01 GM34921 (to S. S. T). The authors declare that they have no conflicts of interest with the contents of this article. The content is solely the responsibility of the authors and does not necessarily represent the official views of the National Institutes of Health.

This article has been selected as one of our Editors' Picks.

[1] Supported by fellowships from CONACyT (Consejo Nacional de Ciencia y Tecnología, Mexico).

[2] Supported by the National Institutes of Health/NCI Grant CA221289.

[3] To whom correspondence should be addressed: Dept. of Pharmacology, CINVESTAV-IPN, Av. Instituto Politécnico Nacional 2508, Col. San Pedro Zacatenco, 07360 Mexico City, Mexico. Tel.: 52-55-5747-3380; Fax: 52-555747-3394; E-mail: jvazquez@cinvestav.mx.

[4] The abbreviations used are: C, catalytic; R, regulatory; PKA, protein kinase A; RacGEF, Rac guanine exchange factor; P-REX1, phosphatidylinositol 3,4,5-trisphosphate-dependent Rac exchange factor 1; AKAP, A kinase-anchoring protein; ANOVA, analysis of variance; DMEM, Dulbecco's modified Eagle's medium; FBS, fetal bovine serum; PAE, porcine aortic endothelial cell; IBMX, isobutylmethylxanthine; siEGFP, short-interfering enhanced green fluorescent protein; CNB-B, cyclic nucleotide-binding domain B; PGE_2, prostaglandin E_2; S1P, sphingosine 1-phosphate; CREB, cAMP-response element-binding protein; ACRO, acrodysostosis; PIP_3, phosphatidylinositol 3,4,5-trisphosphate; PKAS, phospho-PKA substrate antibody; FBS, fetal bovine serum; DAPI, 4,6-diamidino-2-phenylindole; GST, glutathione *S*-transferase; DEP, Dishevelled, EGL-10, and Pleckstrin domain; DH, Dbl homology domain; PH, pleckstrin homology domain; esiRNA, endoribonuclease-prepared siRNA; 6-Bnz, N^6-benzoyladenosine 3′,5′-cyclic monophosphate; 8-AHA, 8-(6-aminohexyl)aminoadenosine-3′,5′-cyclic monophosphate.

quently including AKAPs themselves as part of regulatory feedback loops (4). AKAP-Lbc and α4 integrins are examples of those interacting proteins involved in cell migration (5, 6).

Strikingly, the kinase-independent signaling potential of cAMP-bound PKA regulatory subunits remains poorly understood. Recently, we reported that type Iα PKA regulatory subunit (RIα) interacts with P-REX1, a chemotactic RacGEF, via the cyclic nucleotide-binding domain B (CNB-B) of RIα that establishes noncanonical interactions with P-REX1–PDZ domains. Signaling via G_i-coupled CXCR4 receptors promotes P-REX1 translocation to the plasma membrane that mobilizes RIα in the process. The direct regulatory role that PKA catalytic subunits exert on P-REX1 occurs by phosphorylation of P-REX1 at its DEP1 domain, on serine 436, promoting intramolecular inhibitory interactions between the phosphorylated DEP domain and the catalytic DH-PH cassette (7). Here, we expand our understanding of P-REX1 regulation by PKA by providing evidence that supports a novel mechanism of cAMP-dependent P-REX1 activation via RIα. The emerging model indicates a dual ability of PKA to regulate separated and independent P-REX1 protein pools, stimulating a fraction of this chemotactic RacGEF via direct interaction with regulatory subunits and restricting other fractions by phosphorylation-dependent inhibition. Moreover our results reveal novel signaling features of PKA regulatory subunits, beyond their regulatory role on their kinase counterparts, directly acting as cAMP-dependent transducers.

Results

EP2 prostaglandin receptors promote interaction of endogenous PKA–RIα with active P-REX1 and endothelial cell migration

We have previously demonstrated that PKA phosphorylates P-REX1 at Ser-436 promoting inhibitory intramolecular interactions (7). In addition, we reported that the regulatory subunits of type I PKA directly interact with P-REX1 increasing the potential mechanisms by which PKA might regulate this multidomain RacGEF. Specifically, RIα– cAMP-binding domains, particularly CNB-B, establish noncanonical interactions with P-REX1, raising the possibility that RIα might play a direct cAMP-dependent and kinase-independent effect on P-REX1. Thus, hypothetically, PKA catalytic and regulatory subunits might fine-tune P-REX1 activity by a dual-regulatory input (Fig. 1*A*) or target different P-REX1 molecules. To start addressing these possibilities, with emphasis on the potential positive role of RIα on P-REX1, we studied the effects of endogenous EP2 receptors in endothelial cells. EP2 is a prostaglandin E_2 (PGE_2) receptor described as a G_s-coupled angiogenic receptor (8). We addressed EP2-dependent effects on cell migration, actin cytoskeleton reorganization, P-REX1 and Rac activation, and the interaction of RIα with active P-REX1. As control, we confirmed the effect of the EP2-signaling pathway on PKA activity as evidenced by the phosphorylation of CREB, a prototypic PKA substrate. We initially validated the functional and signaling properties of EP2 in porcine aortic endothelial cells (PAE). We found that PGE_2 and butaprost, an EP2-specific agonist, stimulated PAE cells to migrate in two different experimental systems, wound-healing assays and chemotactic assays in Boyden chambers (Fig. 1, *B* and *C*, respectively). These results correlated with PGE_2-induced actin cytoskeleton remodeling promoting endothelial cell extension (Fig. 1*D*), similar to the effect observed in response to sphingosine 1-phosphate (S1P) (Fig. 1*D*), suggesting the activation of the P-REX1/Rac signaling axis. In cell migration experiments, serum (Fig. 1*B*), sphingosine 1-phosphate, and hepatocyte growth factor (Fig. 1*C*) were used as positive controls. In these cells, PGE_2 and butaprost also promoted CREB phosphorylation on serine 133, a residue known to be phosphorylated by PKA (Fig. 1, *E* and *F*), suggesting the coupling of this receptor to G_s and the cAMP–PKA signaling pathway. Next, we directly tested the effect of EP2 activation on the P-REX1/Rac signaling axis. Butaprost promoted Rac (Fig. 1*G*) and P-REX1 activation (Fig. 1*H*), in very similar kinetics. As we previously reported an interaction and reciprocal regulation between P-REX1 and PKA, we had particular interest on the dynamics of P-REX1 and PKA interaction. Then, we looked for the association of PKA subunits with the fraction of active P-REX1, isolated by pulldown with recombinant nucleotide-free Rac. Interestingly, we found endogenous RIα PKA-regulatory subunit interacting with active P-REX1 (Fig. 1*H*, *2nd blot, PD*), whereas the catalytic Cα subunit was undetectable. Thus, we hypothesized that PKA might have a positive role on P-REX1 signaling, mechanistically explained by the effect of cAMP-promoted direct interaction between RIα and P-REX1, leading to P-REX1 activation (Fig. 1*A*).

Direct stimulation of type I PKA promotes P-REX1 activation

Because we observed that G_s-coupled EP2 receptors simultaneously activated PKA and P-REX1 and coincidently promoted the interaction between RIα and the active fraction of P-REX1, we decided to explore whether P-REX1 could be activated in response to direct stimulation of type I PKA. Thus, we used two cAMP analogs 6Bnz/8AHA-cAMP (9), which combined are specific for RIα (Fig. 2*A*), and we evaluated their effect as activators of endogenous Rac and P-REX1 in endothelial cells. We found that stimulation of type I PKA led to activation of endogenous Rac and P-REX1 (Fig. 2, *B* and *C*, respectively). Moreover, we detected that these cAMP analogs promoted interaction of endogenous RIα with active P-REX1 (Fig. 2*C*, *PD, 2nd panel*). As expected, direct activation of type I PKA led to CREB phosphorylation in endothelial cells (Fig. 2, *B* and *C*) as well as in HEK293T cells (Fig. 2*D*). Since we previously demonstrated a phosphorylation-dependent inhibitory effect of the P-REX1 C-region on P-REX1 activity (7), we assessed whether the positive effect of RIα-specific cAMP analogs on P-REX1 could be restricted to the N-region of P-REX1 containing the DH-PH cassette and the two DEP and two PDZ regulatory modules. We measured the effect of exclusive stimulation of type I PKA on P-REX1 activity in HEK293T cells expressing FLAG–P-REX1–DH–PDZ2. As in the case of endogenous P-REX1 activation in endothelial cells, we observed a similar increase in FLAG–P-REX1–DH–PDZ2 activity and detected endogenous RIα associated with the isolated fraction of active FLAG–P-REX1–DH–PDZ2 (Fig. 2*D*). Interestingly, although the absence of P-REX1 C-region led to a high basal amount of active P-REX1, the RIα-specific cAMP analogs still had a significant

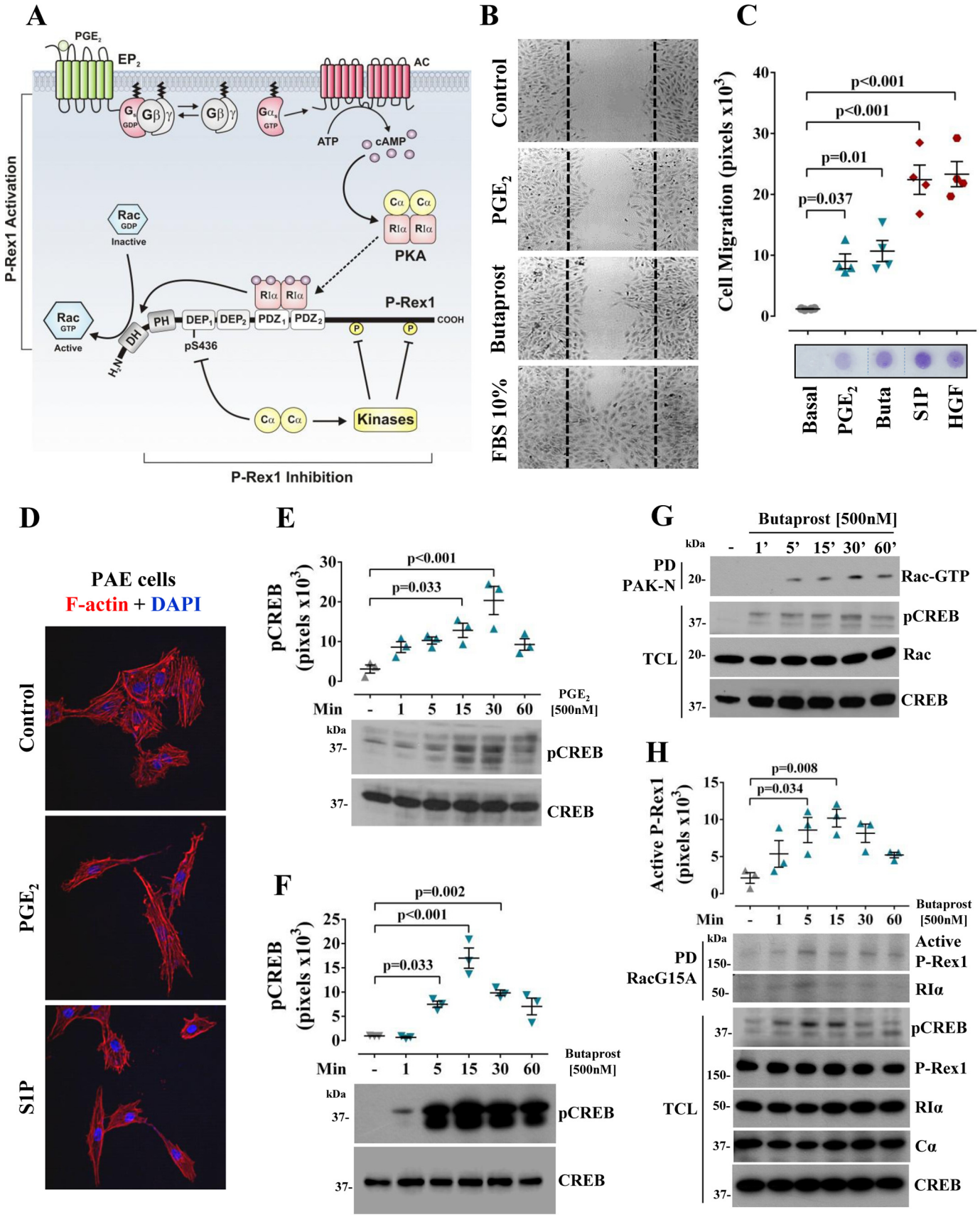
A
PGE2
EP2
AC
ATP
cAMP
PKA
Rac GDP Inactive
Rac GTP Active
P-Rex1
PH
DEP1
DEP2
PDZ1
PDZ2
COOH
pS436
Kinases
P-Rex1 Activation
P-Rex1 Inhibition
B
Control
PGE2
Butaprost
FBS 10%
C
Cell Migration (pixels x10^3)
p<0.001
p<0.001
p=0.01
p=0.037
Basal
PGE2
Buta
S1P
HGF
D
PAE cells
F-actin + DAPI
Control
PGE2
S1P
E
pCREB (pixels x10^3)
p<0.001
p=0.033
Min
PGE2 [500nM]
pCREB
CREB
F
pCREB (pixels x10^3)
p=0.002
p<0.001
p=0.033
Butaprost [500nM]
pCREB
CREB
G
Butaprost [500nM]
1' 5' 15' 30' 60'
PD PAK-N
Rac-GTP
pCREB
TCL
Rac
CREB
H
Active P-Rex1 (pixels x10^3)
p=0.008
p=0.034
Butaprost [500nM]
PD RacG15A
Active P-Rex1
RIα
pCREB
TCL
P-Rex1
RIα
Cα
CREB

effect that also coincided with an increased association of endogenous RIα (Fig. 2*D*, *PD*). These results support the existence of a cAMP → PKA → P-REX1 signaling axis in which RIα interaction with P-REX1 contributes to the activation of this RacGEF.

P-REX1 activation by type I PKA is linked to its interaction with RIα

Previously, using the yeast two-hybrid system, we identified a fraction of RIα, corresponding to its second cAMP-binding domain, as a specific interactor of P-REX1–PDZ domains (7). Thus, the complex of P-REX1 with RIα is reminiscent of guanine exchange factors directly activated by cAMP, which are structurally characterized by the presence of DEP and cAMP-binding domains (10). Because our previous results indicated that in endothelial cells endogenous G_s-coupled EP2 receptors that stimulate type I PKA lead to P-REX1 activation coincidently with its interaction with RIα, we hypothesized that RIα–P-REX1 interaction could directly be stimulated by cAMP. Consistent with this possibility, pharmacological activation of adenylate cyclase (with forskolin) promoted the interaction between endogenous RIα and P-REX1 in PAE cells (Fig. 3*A*, *upper panel, IP-RIα*), coincident with the activation of PKA detected by the phosphorylation of CREB (Fig. 3*A*, *pCREB in TCL*). Similarly, in HEK293T cells, adenylate cyclase stimulation with forskolin and RIα-specific cAMP analogs led to a robust interaction between endogenous RIα and P-REX1–DH–PDZ2, expressed as a GST construct lacking the inhibitory C-region, detected by pulldown experiments (Fig. 3, *B* and *C*, respectively). Remarkably, the Z6 construct, the original clone identified as a P-REX1 interactor in the yeast two– hybrid system, having an isolated RIα CNB-B domain, increased its binding to P-REX1 PDZ-PDZ tandem in response to forskolin stimulation (Fig. 3*D*, *upper panel*), indicating that the CNB-B domain is a structural determinant for the cAMP-dependent binding of RIα to P-REX1. To gain further insight into the role of cAMP-binding domains on the interaction between RIα and P-REX1, we analyzed the potential of RIα CNB-B mutants (Fig. 3*E*) as P-REX1 interactors and activators. In HEK293T cells, we expressed wildtype RIα (WT) or RIα mutants, R335K, and acrodysostosis (ACRO(1–365)) characterized by perturbations on the CNB-B domain (cAMP-resistant), together with GST–P-REX1–PDZ–PDZ domains, and we assessed their interaction by pulldown. Highlighting the importance of CNB-B in the interaction between RIα and P-REX1 PDZ domains, we found that both RIα mutants, R335K and especially the ACRO, exhibited a better interaction with P-REX1 PDZ domains than WT RIα (Fig. 3*F*); however only the ACRO mutant had a discrete but consistent effect on P-REX1 activation (Fig. 3*G*). The coincident effect of the ACRO mutant as a better interactor and activator of P-REX1 suggested that P-REX1 activation indeed depended on its interaction with RIα, but also a particular conformation at the CNB-B domain seems relevant.

P-REX1 activation by type I PKA depends on regulatory but not catalytic subunit expression

Because P-REX1 activation correlated with its interaction with RIα, stimulated by cAMP, we assessed whether knockdown of type I PKA regulatory or catalytic subunits had an effect on P-REX1 activation. Using esiRNAs (a mixture of siRNAs targeting a fraction of 436 nucleotides within the 6633-nucleotide length of P-REX1 mRNA), we decreased P-REX1 expression in MCF7 cells and observed that P-REX1 knockdown prevented the effect of 6Bnz/8AHA-cAMP, type I PKA-specific analogs, as promoters of Rac activation (Fig. 4*A*). These results indicated that stimulation of type I PKA requires P-REX1 to activate Rac. In contrast, the catalytic kinase activity of type I PKA was not influenced by a reduced expression of P-REX1, as demonstrated by the phosphorylation of CREB in response to 6Bnz/8AHA-cAMP in P-REX1 knockdown cells (Fig. 4*A*). Similarly, using RIα- or Cα-specific esiRNAs, we observed that decreased expression of RIα but not Cα prevented P-REX1 activation in response to type I PKA stimulation (Fig. 4*C*). As expected, Cα knockdown prevented the phosphorylation of CREB (Fig. 4*C*, *2nd panel*). Consistent with previous reports, we observed that PKA Cα knockdown also decreased RIα expression (11). Furthermore, to confirm the specific effect of esiRNAs, we transfected individual siRNAs that target P-REX1 (3625 and 3809) or RIα (740 and 175). EGFP and β-Gal siRNAs were used as controls. These P-REX1 and RIα siRNAs efficiently decreased the expression of their targets and similarly abrogated their respective contribution on PKA-dependent Rac and P-REX1 activation (Fig. 4, *B* and *D*, respectively) without significant alteration on CREB phosphorylation by the PKA Cα subunits. These results further support the idea that

Figure 1. EP2 prostaglandin receptors promote endothelial cell migration, P-REX1/Rac activation, and interaction of endogenous PKA–RIα with active P-REX1. *A*, working hypothesis postulating that P-REX1 activity is fine-tuned by independent actions of type I PKA regulatory and catalytic subunits. Accordingly, G_s-coupled EP2 receptor activates P-REX1 via cAMP-dependent direct interaction with regulatory subunits and eventually, as we previously described (7), inhibited by phosphorylation leading to intramolecular inhibitory interactions. *B*, PGE_2 (1 μM) and butaprost (1 μM) (a specific EP2 agonist) promote migration of PAE cells in wound-healing assays. The pictures represent the wound closure of PAE cells after 16 h of stimulation, and S1P (1 μM) and 10% FBS were used as positive controls. Three independent experiments were performed ($n = 3$). *C*, PGE_2 (1 μM) and butaprost (1 μM) promote chemotactic migration of PAE cells in Boyden Chamber Chemotaxis assays; S1P (1 μM) and HGF (10 ng/ml) were used as positive controls. *Graph* shows the densitometric analysis of four independent chemotaxis assays ($n = 4$). Data were analyzed by one-way ANOVA followed by Tukey's multiple comparison test, and *p* value is indicated. *D*, effect of EP2 activation on actin cytoskeleton reorganization in PAE cells was assessed with phalloidin staining. PAE cells, starved for 16 h, were stimulated with PGE_2 (1 μM) and S1P (1 μM) for 15 min, and DAPI was used to show the nuclei. Images are representative of 10 different fields. *E* and *F*, PGE_2 (500 nM) and butaprost (500 nM) promote phosphorylation of PKA substrate CREB at serine 133. Serum-starved PAE cells were stimulated with PGE_2 or butaprost at the indicated times and then lysed and processed for immunoblot against pCREB and total CREB. Graphs show the densitometric analysis of pCREB from three independent experiments ($n = 3$). One-way ANOVA followed by Tukey's multiple comparison test was performed; significant *p* values are indicated. *G*, EP2 stimulation induces Rac activation in endothelial cells. Serum-starved PAE cells were stimulated with butaprost (500 nM) at the indicated times and lysed and processed for pulldown using GST-PAKN beads and analyzed by immunoblot with anti-Rac, pCREB, and total CREB antibodies. *H*, EP2 stimulation promotes P-REX1 activation in endothelial cells. Serum-starved PAE cells were stimulated with butaprost (1 μM) at the indicated times and processed for pulldown assays to capture active P-REX1 using GST–RacG15A beads. Western blottings of anti-P-REX1, PKA–RIα, and Cα were done in pulldowns, and total cell lysates, as well as pCREB and total CREB, were used as control. PKA-Cα was not detected associated with active P-REX1 (not shown). *Graph* shows the densitometric analysis of active P-REX1 from three independent experiments ($n = 3$). One-way ANOVA followed by Tukey's multiple comparison test was performed, and significant *p* values are shown in the *graph*.

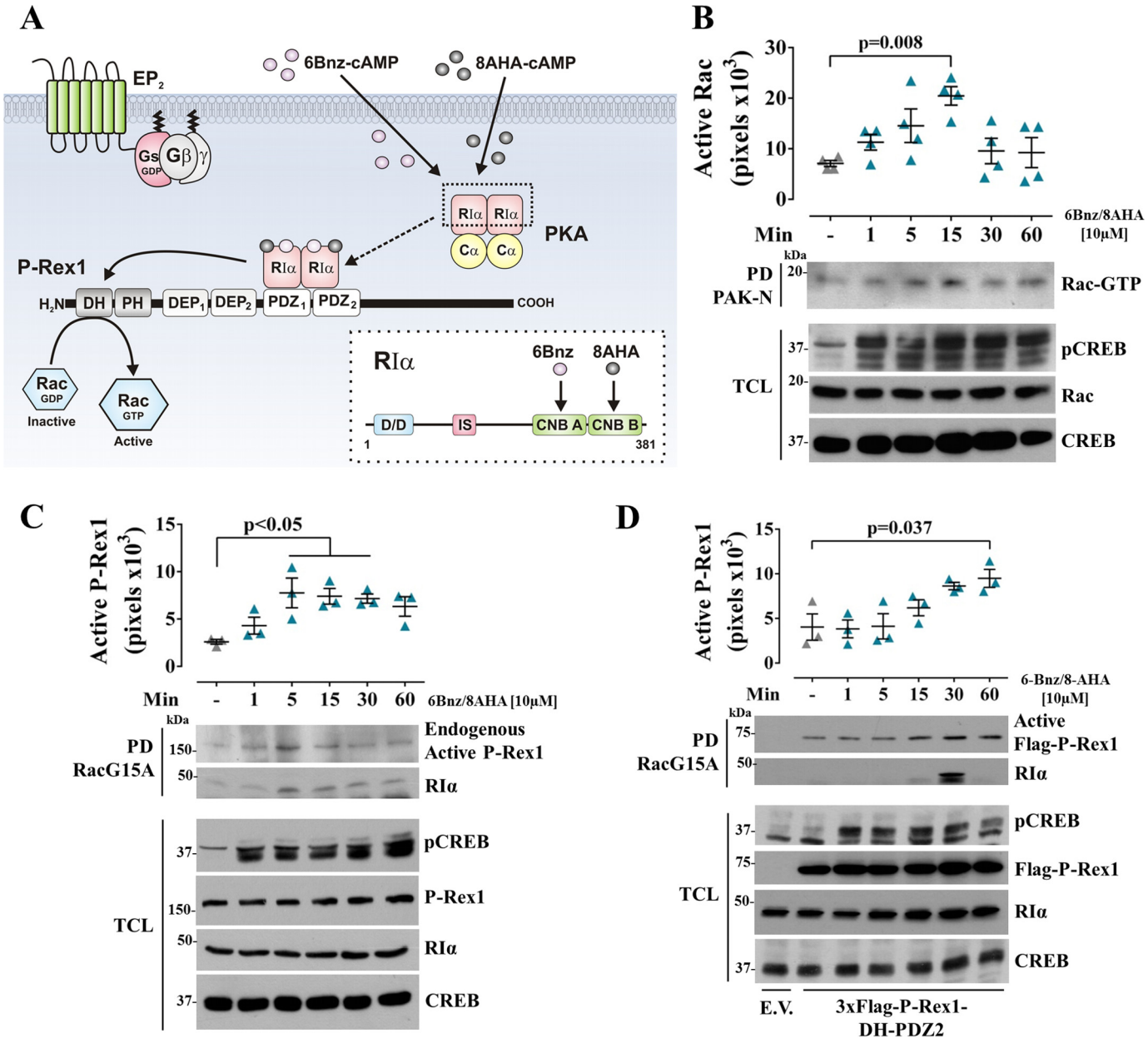

Figure 2. Direct stimulation of type I PKA promotes P-REX1 activation. *A*, hypothetical effect of direct stimulation of type I PKA on P-REX1. *B*, direct stimulation of type I PKA promotes Rac activation in endothelial cells. Serum-starved PAE cells were stimulated at the indicated times with 6-Bnz–cAMP (10 μM) and 8-AHA–cAMP (10 μM) cAMP analogs, and active Rac was isolated with GST–PAKN beads. Total and pCREB were detected by Western blotting in total cell lysates. *Graph* shows the densitometric analysis of four independent experiments of Rac activation ($n = 4$). One-way ANOVA followed by Tukey's multiple comparison test was performed, and significant *p* values are shown in the *graph*. *C*, direct stimulation of type I PKA promotes P-REX1 activation and association of RIα with the active fraction of P-REX1 in endothelial cells. PAE cells were stimulated as indicated in *B*, and active P-REX1 was isolated with GST–RacG15A and detected by immunoblot; RIα was revealed in the pulldown of active P-REX1 and in total cell lysates. pCREB and total CREB revealed in total cell lysates were used as controls. *Graph* shows the densitometric analysis of active P-REX1 from three independent experiments ($n = 3$). One-way ANOVA followed by Tukey's multiple comparison test was performed, and significant *p* values are shown in the *graph*. *D*, P-REX1 lacking the C-terminal region is activated in response to direct stimulation of type I PKA. HEK293T cells expressing FLAG–P-REX1–DH–PDZ2 construct were serum-starved and stimulated with cAMP analogs for type I PKA at the indicated times. Active P-REX1 was isolated with GST–RacG15A beads. Samples were processed for immunoblot against FLAG, RIα, pCREB, and total CREB. *Graph* shows the time course of FLAG–P-REX1 activation from three independent experiments ($n = 3$). One-way ANOVA followed by Tukey's multiple comparison test were performed, and the significant *p* value is shown in the *graph*.

type I PKA controls P-REX1 activity by independent intervention of regulatory and catalytic subunits.

Endogenous P-REX1 preferentially interacts with cAMP-bound RIα and, in vitro, they form an active RacGEF complex

Because pulldown experiments using lysates from cells stimulated with forskolin or RIα-specific cAMP analogs revealed a positive effect of cAMP on the interaction between RIα and P-REX1, we wanted to directly assess the possible preferential interaction of P-REX1 with cAMP-bound RIα. To this end, we used specific cAMP affinity matrices to isolate either RIα or PKA-I holoenzyme from MCF7 cell lysates (12), and we compared whether P-REX1 preferentially remains bound with the fraction of RIα isolated with the cAMP affinity matrix (Fig. 5*A*).

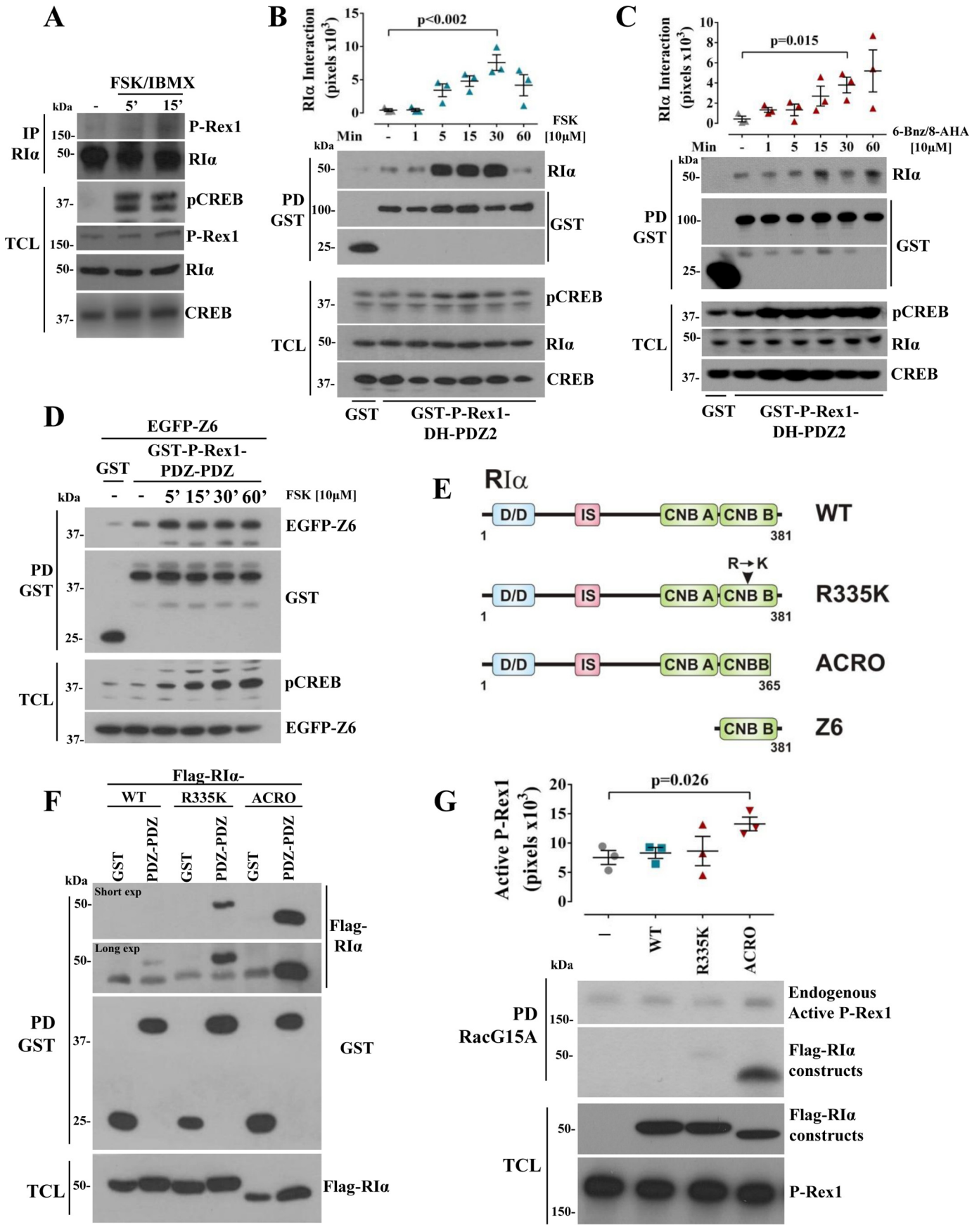
A
FSK/IBMX
kDa
-
5'
15'
IP RIα
150-
50-
P-Rex1
RIα
TCL
37-
150-
50-
37-
pCREB
P-Rex1
RIα
CREB
B
RIα Interaction (pixels x10³)
p<0.002
FSK [10μM]
Min
-
1
5
15
30
60
PD GST
RIα
GST
TCL
pCREB
RIα
CREB
GST
GST-P-Rex1-DH-PDZ2
C
RIα Interaction (pixels x10³)
p=0.015
6-Bnz/8-AHA [10μM]
PD GST
RIα
GST
TCL
pCREB
RIα
CREB
GST
GST-P-Rex1-DH-PDZ2
D
EGFP-Z6
GST
GST-P-Rex1-PDZ-PDZ
FSK [10μM]
5' 15' 30' 60'
PD GST
EGFP-Z6
GST
TCL
pCREB
EGFP-Z6
E
RIα
D/D
IS
CNB A
CNB B
CNBB
1
381
365
WT
R→K
R335K
ACRO
Z6
F
Flag-RIα-
WT
R335K
ACRO
GST
PDZ-PDZ
Short exp
Long exp
Flag-RIα
PD GST
GST
TCL
Flag-RIα
G
Active P-Rex1 (pixels x10³)
p=0.026
–
WT
R335K
ACRO
PD RacG15A
Endogenous Active P-Rex1
Flag-RIα constructs
TCL
Flag-RIα constructs
P-Rex1

As shown in Fig. 5, *B* and *C*, P-REX1 was present in the pulldown of cAMP-bound RIα (isolated with cAMP-agarose) but not in the one used to isolate the PKA-I holoenzyme (with (R_p)-8-AHA-cAMP-agarose). These results indicated that, endogenously, P-REX1 preferentially interacts with the cAMP-bound active RIα rather than with RIα that is part of the type I holoenzyme (Fig. 5, *B* and *C*). Besides, we tested whether direct interaction of purified RIα with P-REX1 is sufficient to activate P-REX1. To confirm this possibility, we first purified bacterial recombinant RIα with cAMP-resin and P-REX1, from HEK293T cells, using the HaloTag system and analyzed their interaction. Both P-REX1 and RIα were detected as single bands by Coomassie staining (Fig. 5*D*). To further confirm that the interaction between cAMP-bound RIα and P-REX1 detected in cell lysates was in fact direct, we incubated purified RIα with purified P-REX1 and subjected them to pulldown assays with cAMP- and (R_p)-cAMP-agaroses. Again, we precipitated RIα with both resins, but P-REX1 was preferentially associated to RIα in the cAMP-resin (Fig. 5*E*). To assess whether *in vitro* RIα and P-REX1 formed an active RacGEF complex, we used recombinant nucleotide-free Rac fused to GST to isolate the putative active RacGEF complex formed by P-REX1 and RIα. We found that RIα did activate P-REX1 and remained associated to the isolated fraction of active P-REX1 (Fig. 5*F*), suggesting that RIα promoted P-REX1 activation by direct interaction.

P-REX1 interaction with PKA–RIα is necessary for EP2-dependent endothelial cell migration

Stimulation of the P-REX1/Rac pathway by RIα suggests the cAMP-dependent interaction of this PKA regulatory subunit with P-REX1 is especially relevant for cell migration elicited by chemotactic G_s-coupled receptors. To test this possibility, we decided to perturb the interaction of RIα with P-REX1 by expressing the P-REX1–PDZ1 domain, mapped as the minimal RIα-interacting domain, to compete the endogenous interaction (Fig. 6*A*). Consistent with previous results (Fig. 3, *A–D*), endogenous RIα interacted with P-REX1–PDZ domains in response to forskolin stimulation (Fig. 6*B*). As predicted, expression of EGFP–P-REX1–PDZ1 domain competed in the interaction between endogenous P-REX1 and RIα isolated by pulldown with cAMP-resin (Fig. 6*C*, *left panel*). Moreover, P-REX1–PDZ1 domain prevented the activation of endogenous P-REX1 in response to direct stimulation of type I PKA, without significantly perturbing PKA catalytic activity measured by CREB phosphorylation (Fig. 6*D*). Notably, in PAE cells expression of the P-REX1–PDZ1 domain decreased the effect of EP2 agonists, but not serum (FBS), on cell migration (Fig. 6, *E* and *F*). These results suggest that EP2 promotes endothelial cell migration via a cAMP–RIα/P-REX1 pathway.

PKA regulatory and catalytic subunits target distinct P-REX1 molecules

The positive effect that RIα exerts on P-REX1 signaling might counteract the inhibitory effect of P-REX1 phosphorylation by PKA Cα subunits. These opposite effects might fine-tune P-REX1 activity or target distinct P-REX1 molecules. To understand the apparent paradoxical effects of PKA on P-REX1, we stimulated EP2 receptors in COS7 cells and isolated active and inactive pools of FLAG–P-REX1 at different times of stimulation. Notably, active P-REX1 molecules, isolated by pulldown with GST–RacG15A, were not phosphorylated (Fig. 7*A*, *PD-RacG15A*), whereas the inactive fraction, isolated by subsequent immunoprecipitation, contained phosphorylated P-REX1, detected by Western blotting with anti-phospho-PKA substrate (PKAS) antibodies (Fig. 7*A*, *IP FLAG*). Our results suggest that upon PKA activation and dissociation, RIα activates nonphosphorylated P-REX1, whereas Cα targets different P-REX1 molecules restricting them by phosphorylation. Eventually, because the fraction of active P-REX1 decreases and the inactive phosphorylated fraction increases (Fig. 7*A*), the dual signaling by PKA leans toward the desensitizing effect on P-REX1 by direct phosphorylation (Fig. 7*B*).

Discussion

P-REX1, a multidomain RacGEF centrally involved in chemotactic G protein– coupled receptor signaling, is synergistically activated by Gβγ and PIP_3 (13–16). Previously, we reported a reciprocal communication between P-REX1 and PKA. Accordingly, P-REX1 localizes PKA RIα to the plasma membrane and PKA inhibits P-REX1 by phosphorylating it (7). In the current study, we extend our understanding of this recip-

Figure 3. P-REX1 activation by type I PKA is linked to its interaction with RIα. *A*, stimulation of the cAMP pathway promotes interaction between endogenous P-REX1 and RIα in endothelial cells. Serum-starved PAE cells were stimulated with forskolin (10 μM) at the indicated times. Then endogenous RIα was immunoprecipitated, and bound P-REX1 was detected by Western blotting. Total P-REX1, RIα, pCREB (stimulation control), and total CREB were revealed in total cell lysates. *B*, stimulation of the cAMP pathway promotes interaction between endogenous RIα and the DH–PDZ2 region of P-REX1. HEK293T cells expressing GST–P-REX1–DH–PDZ2 construct were serum-starved and stimulated with forskolin (10 μM) as indicated. P-REX1–DH–PDZ2 was isolated using GSH-Sepharose beads. Immunoblot was performed against RIα, GST, pCREB (stimulation control), and total CREB. *Graph* shows the time course of forskolin-induced RIα interaction with P-REX1 from three independent experiments ($n = 3$). One-way ANOVA followed by Tukey's multiple comparison test was performed, and significant *p* value is shown in the *graph*. *C*, direct stimulation of type I PKA promotes interaction of RIα with P-REX1. HEK293T cells expressing GST–P-REX1–DH–PDZ2 construct were serum-starved and then stimulated with 6Bnz-cAMP (10 μM) and 8AHA-cAMP (10 μM) as indicated. P-REX1 was isolated by GST pulldown, and samples were analyzed by Western blotting against RIα, GST, pCREB (stimulation control), and total CREB. *Graph* shows the time course of directly activated RIα interacting with P-REX1, from three independent experiments ($n = 3$). One-way ANOVA followed by Kruskal-Wallis test was performed, and significant *p* value is indicated. *D*, stimulation of the cAMP pathway promotes interaction between Z6 construct (RIα CNB-B domain) and the PDZ1–PDZ2 region of P-REX1. HEK293T cells co-expressing EGFP–Z6 and GST–P-REX1–PDZ1–PDZ2 constructs were serum-starved and stimulated with forskolin (10 μM) as indicated. GST–P-REX1–PDZ1–PDZ2 was isolated with GSH-Sepharose beads. Immunoblot was performed against GFP, GST, pCREB (stimulation control), and total CREB. Three independent experiments were performed ($n = 3$). *E*, schematic representation of WT and mutant RIα constructs R335K and acrodysostosis(1–365) and Z6 (CNB-B). *F*, analysis of interaction between WT RIα and mutants at CNB-B domain and P-REX1 PDZ–PDZ module. HEK293T cells co-expressing GST–P-REX1–PDZ1–PDZ2 domains and FLAG–RIα WT or mutants R335K or ACRO were serum-starved, lysed, and prepared for GST pulldown interaction assays as described previously. Immunoblots were performed against FLAG and GST. Three independent experiments were performed ($n = 3$). *G*, RIα ACRO mutant increases P-REX1 activity. MCF7 cells expressing empty vector or RI WT or R335K or ACRO mutants were serum-starved and lysed, and active P-REX1 was isolated with GST–RacG15A beads. Immunoblots were performed for P-REX1 and FLAG. *Graph* shows the densitometric analysis of three independent experiments ($n = 3$). The *p* value obtained by one-tail Student's *t* test comparing control *versus* ACRO is indicated.

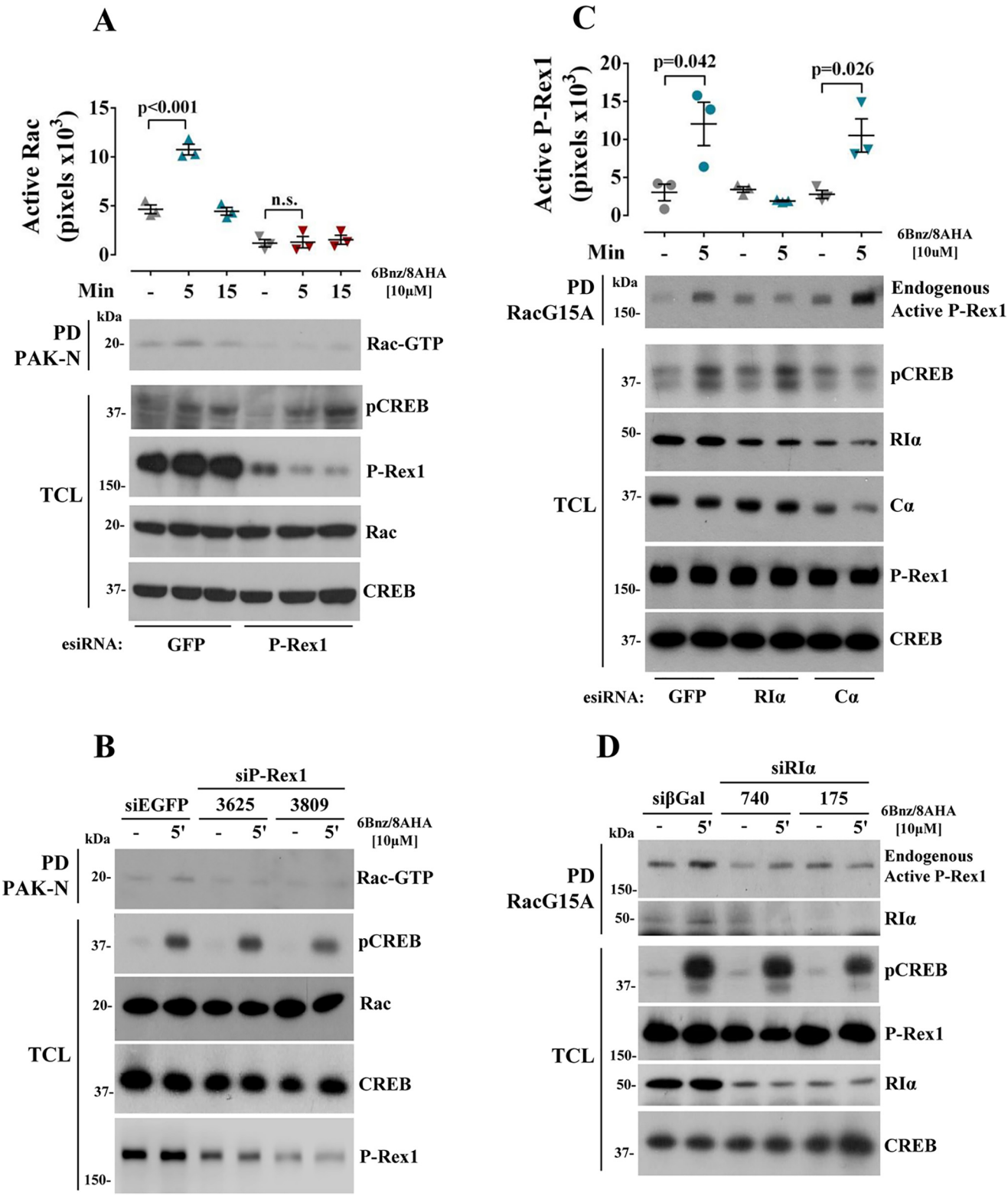

Figure 4. P-REX1 activation by type I PKA depends on regulatory, but not catalytic, subunit expression. *A* and *B*, Rac activation in response to direct stimulation of type I PKA requires P-REX1. MCF7 cells transfected with esiRNAs (*A*) or individual siRNAs (*B*) for P-REX1 or GFP (as negative control) were serum-starved and stimulated at the indicated times with type I PKA-specific cAMP analogs. Active Rac was isolated by pulldown with GST–PAKN and detected by immunoblot. Western blottings in total cell lysates were done for Rac, P-REX1, pCREB, and total CREB. *Graph* in *A* represents the densitometric analysis of three independent experiments ($n = 3$). Two-way ANOVA followed by Tukey test was performed, and significant p value is indicated. *n.s.*, no significant $p > 0.05$. *C* and *D*, P-REX1 activation in response to direct stimulation of type I PKA requires the RIα subunit but not catalytic Cα subunit. MCF7 cells transfected with esiRNAs for PKA–RIα or -Cα subunits (*C*), or siRNAs for PKA–RIα or βGal (as negative control) (*D*), were serum-starved and stimulated with type I PKA-specific cAMP analogs at the indicated times. Active P-REX1 was isolated with GST–RacG15A and detected by immunoblot. Phosphorylation of CREB as well as expression of P-REX1, RIα, Cα, and total CREB were assessed by Western blotting in total cell lysates. *Graph* in *C* represents the densitometric analysis of active P-REX1 from three independent experiments ($n = 3$). One-tail Student's *t* test was performed for the comparisons, and significant p values are indicated.

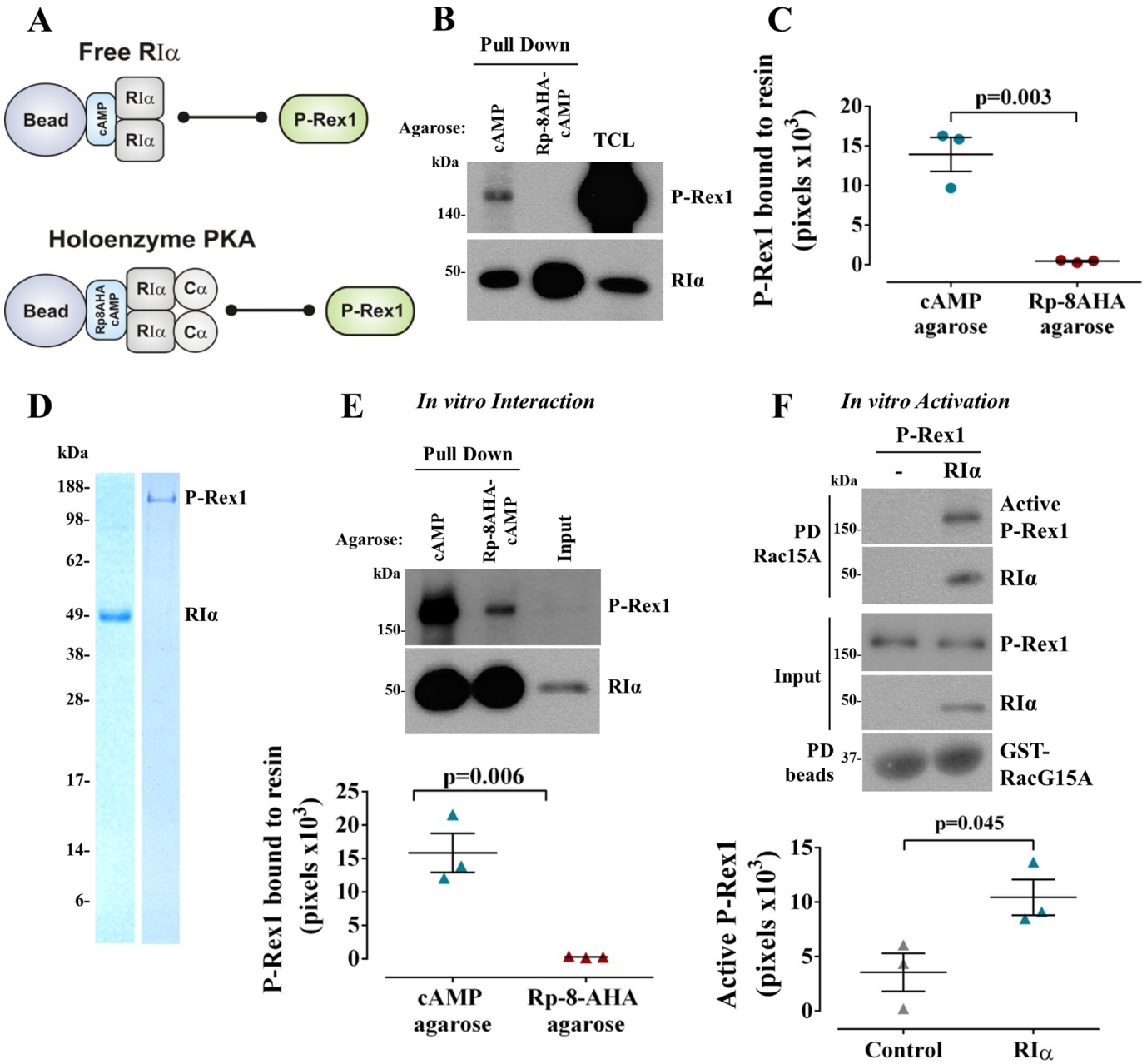

Figure 5. Endogenous P-REX1 preferentially interacts with cAMP-bound RIα, and *in vitro* they form an active RacGEF complex. *A*, drawing shows the experimental strategy to assess whether P-REX1 preferentially interacts with cAMP-bound RIα with respect to type I PKA holoenzyme, isolated by pulldown with affinity matrices containing cAMP or the antagonist analog (R_p)-8AHA-cAMP. *B*, P-REX1 preferentially interacts with free cAMP–RIα but not with inactive PKA holoenzyme. Lysates of serum-starved MCF7 cells were used for pulldown assays with cAMP or (R_p)-cAMP-agaroses. P-REX1 and RIα in the pulldown, and total cell lysate, were detected by Western blotting. *C*, *graph* represents the densitometric analysis of three independent experiments ($n = 3$) like the one shown in *B*. Results were analyzed by one-tail Student's *t* test, and the *p* value is indicated in the *graph*. *D*, Coomassie staining of isolated full-length RIα and P-REX1 used for *in vitro* assays. RIα was expressed in *E. coli* BL21 strain and purified using cAMP-agarose followed by gel filtration. HA–HaloTag–P-REX1, expressed in HEK293T cells, was isolated by pulldown with Halolink resin. P-REX1 was released from the resin using HaloTag–tobacco etch virus protease, removing the HA–HaloTag. *E*, isolated P-REX1 and RIα were incubated *in vitro* and subjected to pull down analysis with cAMP or (R_p)-agaroses. Samples were immunoblotted against P-REX1 and RIα. The *graph* below represents the densitometric analysis of three independent experiments ($n = 3$). Results were analyzed by one-tail Student's *t* test, and *p* value is indicated. *F*, P-REX1 is directly activated by RIα. Purified P-REX1 was incubated in the presence or absence of RIα for 15 min, and the active fraction of P-REX1 was isolated with GST–RacG15A beads. P-REX1 and RIα were detected by immunoblot. Recombinant GST–RacG15A was stained with Ponceau red. The *graph* below represents the densitometric analysis of three independent experiments ($n = 3$). Results were analyzed by one tail Student's *t* test, and *p* value is indicated.

rocal regulation and demonstrate the potential of type I PKA regulatory subunits to directly activate P-REX1. We show that endothelial EP2, a G_s-coupled receptor, promotes P-REX1 activation and interaction of RIα subunit of PKA with the active fraction of P-REX1. This finding is compatible with a previous report showing P-REX1– dependent activation of Rac by β-adrenergic receptors in MCF7 cells (17). EP2 was previously described as a G_s-coupled angiogenic receptor (8); however, the molecular mechanisms by which EP2 stimulates Rho GTPases involved in typical angiogenic responses such as endothelial cell migration, and the identity of RhoGEFs putatively activated downstream of EP2, had remained unknown. Here, we demon-

strated that P-REX1, known to be involved in angiogenic signaling by chemotactic G_i-coupled receptors such as CXCR4 (18, 19), and its effector Rac were activated upon EP2 stimulation, which simultaneously promoted the phosphorylation of CREB, a paradigmatic PKA substrate. Intriguingly, these findings would involve a complex, and apparently paradoxical, mechanism of P-REX1 regulation by PKA. We previously demonstrated that PKA inhibits P-REX1 by promoting phosphorylation-dependent intramolecular inhibitory interactions, and we are now revealing a positive effect of PKA on P-REX1, which is mediated by the RIα subunit. Our current results point to a mechanism depicted in Fig. 7*B* by which PKA regulatory and

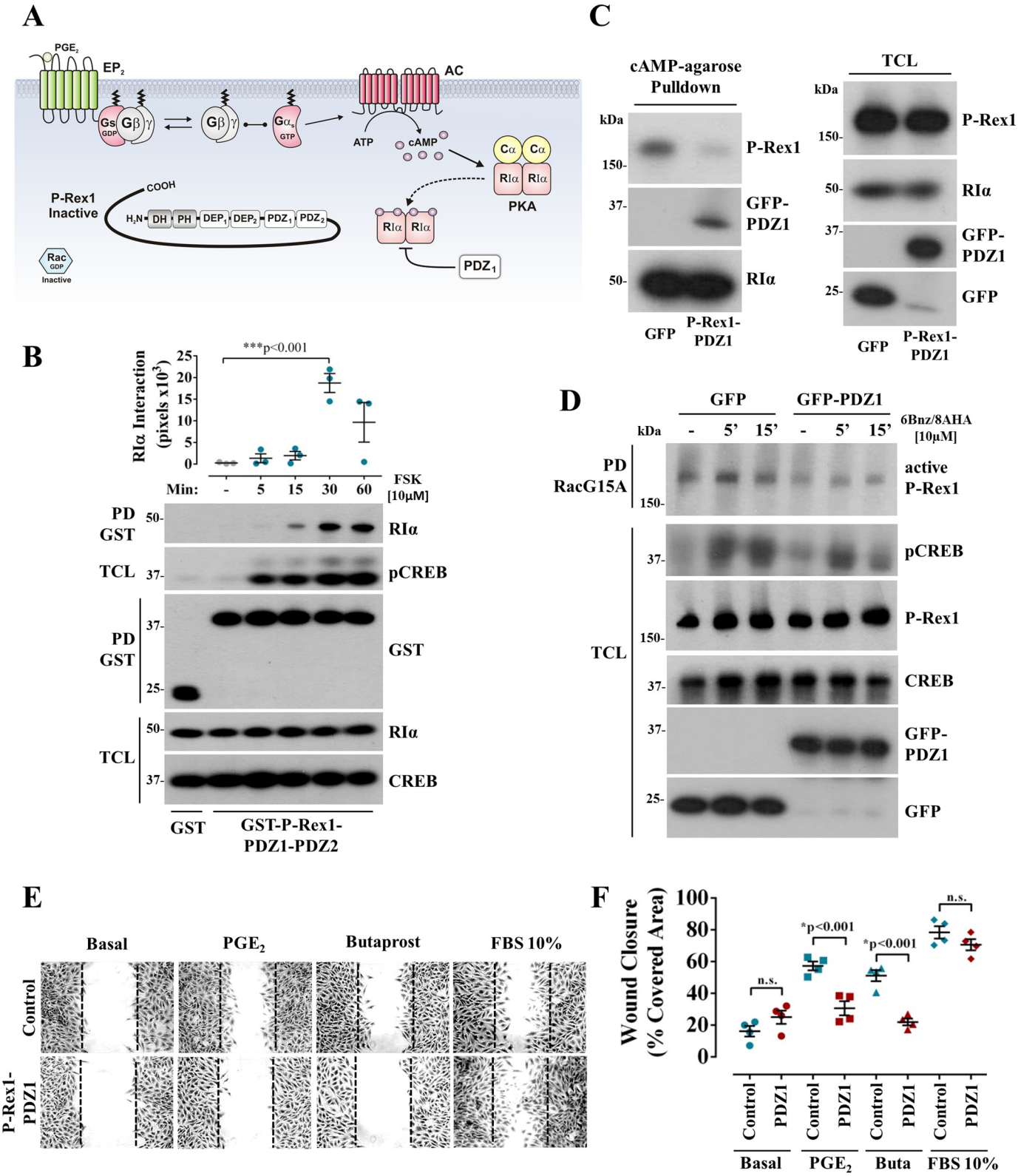

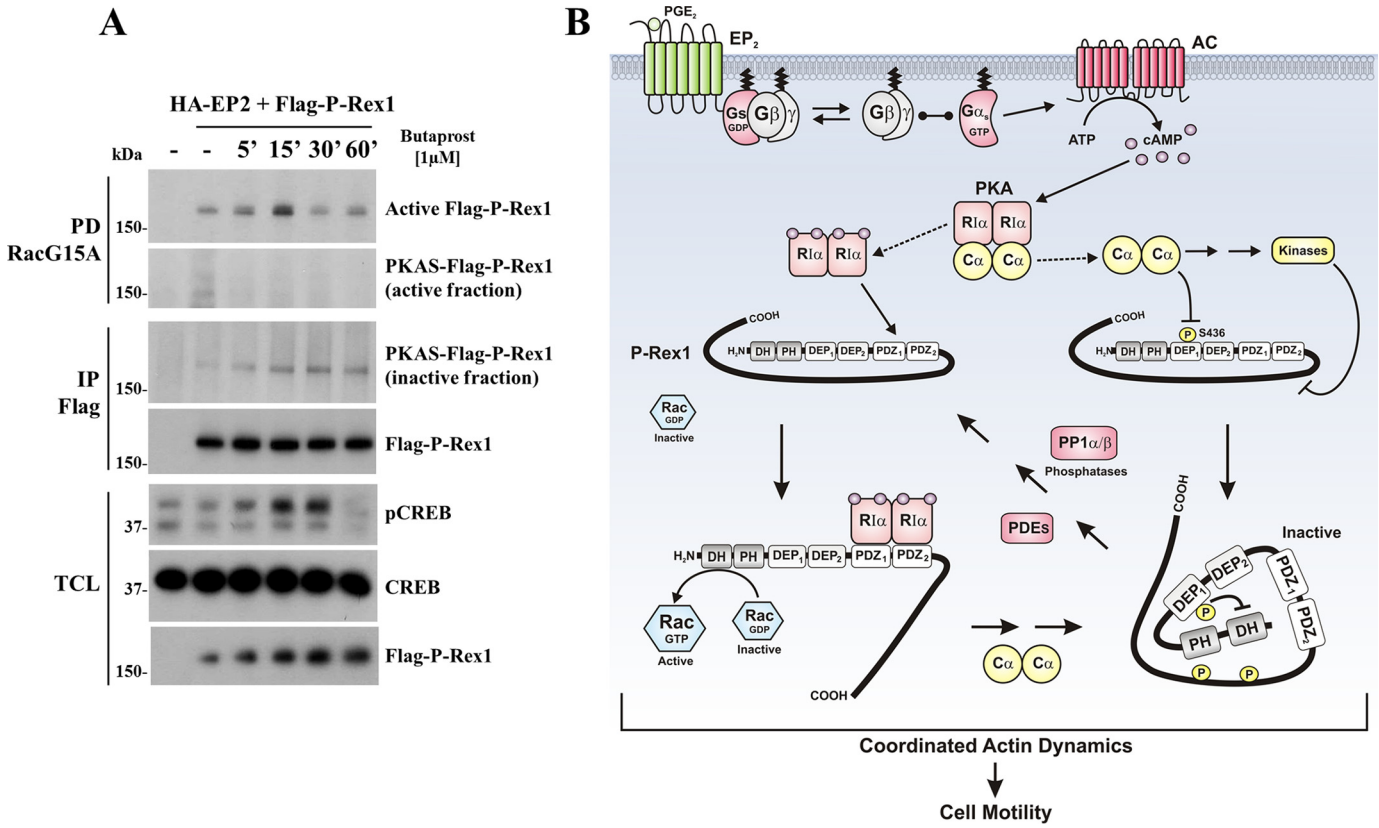

Figure 7. PKA regulatory and catalytic subunits target distinct P-REX1 molecules. *A*, COS7 cells co-expressing 3×HA-EP2 receptors and 3×FLAG–P-REX1 were serum-starved and stimulated with butaprost (1 μM) at the indicated times. Active P-REX1 was isolated with GST–RacG15A beads, and inactive P-REX1 was isolated from supernatants of RacG15A pulldowns by immunoprecipitation with anti-FLAG antibodies. Phosphorylation status of active and inactive P-REX1 was assessed by PKAS. Total cell lysates (*TCL*) were used to reveal pCREB (stimulation control), CREB, and FLAG–P-REX1. Three independent experiments were performed ($n = 3$). *B*, model explaining the effect of PKA regulatory and catalytic subunits on different P-REX1 molecules. G_s-coupled EP2 receptors stimulate adenylate cyclase generating cAMP that binds the RIα subunits of PKA holoenzyme promoting dissociation of cAMP-bound regulatory subunits and active kinase subunits. Based on our results, cAMP–RIα directly activates a fraction of P-REX1 molecules, stimulating GTP loading to Rac (*left,* P-REX1 molecule, stimulatory input). In contrast, PKA Cα subunits phosphorylate and inhibit a distinct pool of P-REX1 (*right,* P-REX1 molecule, inhibitory input). We previously demonstrated that inhibitory phosphorylation of P-REX1 by PKA occurs at Ser-436 on the DEP1 domain and PKA-regulated kinases that phosphorylate the P-REX1 C-terminal region, promoting intramolecular inhibitory interactions (7). Gradually, the fraction of active P-REX1 decreases, and the inactive, phosphorylated form increases, indicating that eventually the PKA Cα inhibitory activity predominates. Later, P-REX1 is taken to its basal state by the intervention of protein phosphatases and cAMP-phosphodiesterases. Overall, our results suggest that P-REX1 activity is fine-tuned by the combined effects of PKA subunits leading to organized cytoskeleton dynamics and effective cell migration.

catalytic subunits would target distinct P-REX1 molecules once they are dissociated in response to signaling pathways stimulating cAMP production.

We demonstrated that cAMP analogs, used as type I-specific PKA agonists, lead to P-REX1 activation coincident with its interaction with the RIα subunit, suggesting that the RIα–P-REX1 interaction, and consequently P-REX1 activation, depend on cAMP binding to RIα. Furthermore, we found that silencing RIα in MCF7 cells prevents P-REX1 activation by RIα-specific cAMP analogs. In contrast, Cα knockdown has no effect on P-REX1 activation but prevents CREB phosphorylation. There are only few documented examples of a positive effect of cAMP

Figure 6. P-REX1 interaction with PKA–RIα is necessary for EP2-dependent endothelial cell migration. *A*, drawing shows the experimental strategy to assess whether P-REX1–PDZ1 domain interferes on the interaction of PKA RIα subunits with P-REX1, preventing RIα-dependent P-REX1 activation and cell migration stimulated by EP2 receptors. *B*, endogenous RIα interacts with P-REX1–PDZ1–PDZ2 domains in a cAMP-dependent manner. HEK293T cells expressing GST–P-REX1–PDZ1–PDZ2 were serum-starved, stimulated with forskolin (10 μM) at the indicated times, and lysed. GST–P-REX1–PDZ1–PDZ2 was isolated with glutathione-Sepharose beads. Immunoblot was performed against RIα, GST, pCREB (stimulation control), and total CREB in pulldowns (*PD GST*) or total cell lysates (*TCL*) as indicated. *Graph* shows the time course of forskolin-induced RIα interaction with P-REX1–PDZ1–PDZ2 from three independent experiments ($n = 3$). One-way ANOVA followed by Tukey's multiple comparison test was performed, and significant *p* value is shown in the *graph*. *C*, P-REX1 PDZ1 domain competes with endogenous P-REX1 for the interaction with RIα pulled down with cAMP-agarose. MCF7 cells expressing EGFP or EGFP–P-REX1–PDZ1 were serum-starved and lysed. Endogenous RIα was isolated with cAMP-agarose beads. RIα, P-REX1, and GFP–PDZ1 in the pulldowns were revealed by immunoblot. Total cell lysates (*TCL, right panel*) were used to confirm the expression of the indicated proteins. Three independent experiments were performed ($n = 3$). *D*, expression of P-REX1–PDZ1 domain prevents P-REX1 activation in response to type I PKA-specific stimulation. MCF7 cells expressing EGFP or EGFP–P-REX1–PDZ1 were serum-starved, stimulated with type I PKA-specific cAMP analogs at the indicated times, and lysed. Active endogenous P-REX1 was isolated using GST–RacG15A beads and revealed by immunoblot. Total cell lysates (*TCL*) were used to detect P-REX1, pCREB (stimulation control), CREB, and GFP. Three independent experiments were performed ($n = 3$). *E*, expression of P-REX1–PDZ1 domain prevents EP2-dependent endothelial cell migration. Confluent PAE cells expressing EGFP or EGFP–P-REX1–PDZ1 were serum-starved and subjected to wound-healing assays. Cells were stimulated with PGE_2 (1 μM) or butaprost (1 μM). Pictures represent the wound closure after 16 h of stimulation; 10% fetal bovine serum (*FBS*) was used as control. *F*, *graph* represents the results of four independent experiments ($n = 4$). Statistical analysis was done by two-way ANOVA followed by Tukey; *p* values are indicated in the *graph*. *n.s.*, no significant $p > 0.05$.

on the association between PKA regulatory subunits and putative signaling effectors. These include RIIβ interacting with Gα_i in response to the coincident activation of G_i- and G_s-coupled receptors, enhancing MAPK signaling (20), and RIα interacting with Bim (B-cell lymphoma family protein), contributing to mitochondria-dependent apoptosis in S49 cells, also involving PKA catalytic activity (21). Consistent with a model in which RIα interacts with P-REX1 and acquires an active conformation that promotes P-REX1 activity, we found that RIα mutants with alterations at their CNB-B domain actually exhibited a better interaction with P-REX1 than WT RIα. However, only the ACRO mutant led to an increased P-REX1 activity, arguing that interaction and conformational adjustments are part of the mechanism by which RIα activates P-REX1. Interestingly, the RIα ACRO mutant is a cAMP-resistant mutant responsible for acrodysostosis, a genetic disease characterized by severe skeletal dysplasia, bone malformations, and hormone resistance (22). Cells expressing RIα ACRO have lower PKA kinase activity. Although the effect on P-REX1 of the cAMP-resistant RIα ACRO contrasts with the observed cAMP-dependent effect of WT RIα, the structure of the monomeric RIα ACRO1 (Lys-92–Ile-365) mutant presents a highly dynamic and disordered C-tail (Arg-357–Ile-365) (23). Because P-REX1 interacts with the CNB-B domain of RIα (Lys-346–Ser-378), the increased flexibility of the RIα ACRO1 (Lys-92–Ile-365) mutant C-tail might contribute to enhance its interaction with P-REX1, having a conformation suitable to activate it. Using peptide arrays, we previously mapped to the C-terminal region (Gly-343–Val-381) of RIα the sequences that interact with P-REX1 (7). Consistent with its increased effect on P-REX1, this region seems to be exposed in the RIα ACRO mutant.

We demonstrated that P-REX1 preferentially interacts with RIα subunits in the presence of cAMP than with the inactive holoenzyme. Moreover, *in vitro*, using purified proteins, RIα is able to directly activate P-REX1. Moreover, EP2-dependent cell migration involves the interaction between RIα and P-REX1, as indicated by the inhibitory effect of the P-REX1 PDZ1 domain, which competes with the interaction and decreases the migratory effect of EP2 receptors. Thus, RIα, as a direct activator of P-REX1, joins the list of upstream regulators of this RacGEF originally including G$\beta\gamma$ and PIP_3 (13). Therefore, P-REX1 could potentially integrate diverse positive combinatorial inputs such as G$\beta\gamma$ + PIP_3, G$\beta\gamma$ + RIα, and PIP_3 + RIα. Remarkably, the co-existence of paradoxical effects of PKA on P-REX1 is explained by independent actions of PKA regulatory and catalytic subunits on distinct P-REX1 protein pools. Considering the known role of RhoGEFs as scaffolds (24), and the increasing number of P-REX1–interacting partners (25–28), our results support the idea that P-REX1 integrates multiple inputs and establishes the basis for a prototypic activation model for this family of multidomain RacGEFs. Additional possibilities include the potential direct regulation between P-REX1–binding partners. For instance, the mechanistic/mammalian target of rapamycin, an upstream regulator of P-REX1 (28), has been reported to be regulated by RIα (29). Moreover, because P-REX1 is in fact a PKA substrate, it could potentially influence cAMP-dependent holoenzyme dissociation and reassembly in which, in the case of type I PKA, it has been documented that substrates play a role in the regulatory circuit of PKA activity (30).

Altogether, our results extend our current view of how PKA and P-REX1 are reciprocally regulated. The emerging picture includes a cAMP-dependent positive role of RIα directly activating a fraction of P-REX1 molecules downstream of chemotactic G_s-coupled receptors. In our model (Fig. 7*B*), PKA activation by G_s signaling and cAMP formation stimulates the activity of a pool of P-REX1 molecules via direct interaction with cAMP–RIα subunits, and another P-REX1 pool is phosphorylated and inhibited by PKA Cα subunits. Gradually, PKA Cα catalytic activity prevails and desensitizes P-REX1 signaling by phosphorylation at Ser-436 and the action of PKA-regulated kinases targeting the C-terminal region (7). Eventually, P-REX1 basal state is restored by protein phosphatases, like PP1α, and cAMP–phosphodiesterases (31). Our results also contribute to define a new paradigm in which PKA regulatory subunits emerge as signaling proteins able to stimulate their own specific effectors via cAMP-dependent direct protein–protein interactions.

Experimental procedures

Plasmids and cDNA constructs

Plasmids have been previously described: pCDNA3.1–FLAG–RIα WT, R335K, and acrodysostosis mutant (1–365) (23); pCEFL–GST-, FLAG-, and HA-tagged P-REX1 constructs and pmCherry-RIα (7); and pCDNA3–EP2 (32). pCEFL–EGFP–P-REX1–PDZ1 construct was prepared by subcloning P-REX1 PDZ1 cDNA from pCEFL-GST–P-REX1–PDZ1 to pCEFL–EGFP vector by restriction with BamHI/EcoRI enzymes. pCEFL–HA–HaloTag–P-REX1, full-length construct, was prepared amplifying HaloTag sequence from pHTN–HaloTag vector using the following primers: 5′cgttcctgattacgctagcATGGCAGAAATCGGTACTGGC3′ and 3′GCTGGGCGCCTCCATgctagcGCTCTGAAAGTACAGATCC5′. The HaloTag cDNA fragment was inserted by Gibson Assembly (New England Biotechnology) into pCEFL–HA–P-REX1, between the HA and P-REX1 sequences, by restriction with NheI enzyme. The construct was confirmed by sequencing.

Cell culture, transfection, and stimulation

HEK293T, COS7, MCF7 and porcine aortic endothelial (PAE) cells were maintained in Dulbecco's modified Eagle's medium (DMEM, Sigma) supplemented with 10% bovine fetal serum. Cells were either transfected using Lipofectamine Plus reagent (Invitrogen) for HEK293T and COS7 cells, PolyFECT (Qiagen) for PAE cells, and Turbofect (ThermoFisher Scientific) or Lipofectamine RNAiMAX (Invitrogen) for MCF7 cells, according to the manufacturer's protocol. Experiments were done 48 h after transfection with plasmids or 72 h after esiRNA or siRNA for knockdown experiments. When indicated, HEK293T, PAE, and COS7 cells were starved for 16 h with serum-free DMEM before stimulation; MCF7 cells were starved for 24 h. For EP2 receptor stimulation, we used prostaglandin E_2 (Sigma, P5640) or butaprost, an EP-specific agonist (Sigma, B6309). Type I PKA was directly stimulated with a combination of cAMP analogs (9): 6-Bnz-cAMP (Sigma, B4560) and

8-AHA-cAMP (Sigma, A2104) that target the CNB-A and CNB-B domains of RI subunits, respectively. As positive controls, we used sphingosine 1-phosphate (Sigma, S9666), hepatocyte growth factor (R&D Systems, 294-HGN), and fetal bovine serum.

Knockdown of P-REX1 and type I PKA subunits

Reverse transfection of MCF7 cells was performed with Lipofectamine RNAiMAX and 30 pmol of esiRNA or individual siRNA. The esiRNAs used were esi-P-REX1 (Sigma, EHU136571), esiRNA-PKA–RIα (Sigma, EHU071341), esiRNA-PKA-Cα (Sigma, EHU132541), or esiRNA-EGFP (Sigma, EHUEGFP), as control. This system includes a pool of multiple siRNAs (esiRNAs are endoribonuclease-prepared siRNAs, all directed toward a fraction of the target mRNA). Individual siRNAs were obtained from Sigma; their sequences were siP-REX1–3625 GAGAUGAGCUGCCCUGUGA, siP-REX1–3809 GAAAGAAGAGUGUACAAUC, siβGal-2891 GGACGCGCGAAUUGAAUUA, siEGFP GCCACAACGUCUAUAUCAU, siRIα-175 CCAUGGAGUCUGGCAGUAC, and siRIα-740 UGAAUGGGCAACCAGUGUU. Lipofectamine and esiRNA or siRNA mixes were prepared in OptiMEM, according to the manufacturer's instructions. Cells were trypsinized and suspended in DMEM containing 5% FBS without antibiotics, and then Lipofectamine/esiRNA complexes were added, and cells were seeded on p60 dishes and incubated overnight at 37 °C in a 5% CO_2 atmosphere. Next day, cells were washed with PBS and cultured with DMEM containing 10% FBS and antibiotics. Experiments with knockdown cells were done 72 h after transfection. Cells were starved in serum-free media for 24 h before being stimulated for 5 min with cAMP analogs 6-Bnz and 8-AHA-cAMP (10 μM).

Pulldown and immunoprecipitation

Cells grown in 35- or 60-mm dishes were washed with cold phosphate-buffered saline (PBS), lysed in 1 ml of ice-cold lysis buffer (50 mM Tris, 150 mM NaCl, pH 7.5, containing 1% Triton X-100, 5 mM EDTA), protease inhibitors (1 mM phenylmethylsulfonyl fluoride, 10 μg/ml leupeptin, and 10 μg/ml aprotinin), and phosphatase inhibitors (1 mM NaF, 1 mM sodium orthovanadate, and 1 mM β-glycerol phosphate), and incubated for 10 min on ice. Cell lysates were centrifuged at 13,000 rpm for 10 min at 4 °C. For immunoprecipitation, supernatants were incubated with 3 μl of RIα antibody or 4 μl of FLAG antibody (for 3× FLAG-tagged P-REX1) and incubated overnight at 4 °C on a rocking platform, and then 35 μl of protein G–agarose beads (Millipore) were added and incubated for 3 h. Samples were centrifuged at 5000 rpm for 2 min at 4 °C, and beads were washed three times with lysis buffer. Finally, beads were resuspended in 1× Laemmli sample buffer containing mercaptoethanol and boiled for 5 min. For pulldown assays of GST-tagged proteins, cell lysates were incubated with 25 μl of GSH-Sepharose beads (GE Healthcare, catalog no. 17-5279-01) for 30–45 min and processed as described for immunoprecipitations. To isolate free RIα or PKA holoenzyme cyclic nucleotides, agaroses were used for pulldowns. MCF7 cell lysates were prepared with 50 μM IBMX and then incubated with 20 μl of cAMP-agarose (Sigma, catalog no. A0144) or (R_p)-8-AHA-cAMP-agarose (MyBioSource catalog no. MBS256231) for 12 h at 4 °C. Samples were centrifuged at 5000 rpm for 2 min at 4 °C, and beads were washed three times with lysis buffer. Finally, beads were resuspended in 1× Laemmli sample buffer containing mercaptoethanol, boiled for 5 min, and processed as described for immunoprecipitations.

Immunoblotting

Cell lysates, pulldown, and immunoprecipitation samples were resolved in SDS-PAGE and transferred to Immobilon membrane (Millipore). Proteins were detected by Western blotting using antibodies with the following specificity: FLAG (Sigma, catalog no. F3165); P-REX1 (catalog no. HPA001927 from Sigma and catalog no. 13168S from Cell Signaling Technology); PKA regulatory subunit (R1α) (catalog no. 610165 from BD Transduction Laboratories and catalog no. 4782S from Cell Signaling Technology); PKA catalytic subunit (Cα) (catalog no. 5675S Cell Signaling Technology); Rac1 (catalog 610651 BD Transduction Laboratories); GST (B-14, Santa Cruz Biotechnology); phospho-(S/T)-PKA substrates (Cell Signaling catalog no. 9621S); phospho-CREB Ser-133 (Cell Signaling catalog no. 9191); and CREB (Cell Signaling catalog no. 9197S). Secondary antibodies were goat anti-mouse monoclonal (Zymed Laboratories Inc., Invitrogen, or KPL) or goat anti-rabbit (Rockland Immunochemicals or KPL).

Rac1 activation assay

Activation of Rac1 was assessed by detecting its interaction with the CRIB domain of PAK fused to GST using a pulldown strategy. PAE and MCF7 cells grown in 60-mm Petri dishes were starved and stimulated (as indicated in figure legends), washed with PBS containing 10 mM $MgCl_2$, and lysed with 0.5 ml of ice-cold lysis buffer containing 10 mM $MgCl_2$. Cell lysates were incubated on ice with 30 μl of GST–PAK CRIB beads for 30 min on a shaker. Beads were then centrifuged at 5000 rpm for 1 min and washed three times with lysis buffer. Beads were then resuspended in 20 μl of 1× Laemmli buffer, boiled for 5 min, centrifuged at 13,000 rpm for 1 min. Beads were then resolved in a 12% acrylamide, transferred to polyvinylidene difluoride membranes, and immunoblotted using anti-Rac1 monoclonal antibodies. As controls, total cell lysates were analyzed in parallel.

Activation of P-REX1

Serum-starved cells, stimulated as indicated in figure legends, were used to detect the activation of P-REX1 assessed by its interaction with nucleotide-free Rac using a pulldown strategy with nucleotide-free recombinant GST–RacG15A essentially as described for Net1 by García-Mata and co-workers (33).

Isolation of active and inactive fractions of FLAG–P-REX1

To address the phosphorylation status of active and inactive fractions of P-REX1, COS7 cells co-expressing EP2 receptors and P-REX1 (3×HA-EP2 and 3×FLAG–P-REX1) were stimulated with butaprost and subjected to pulldown assays with nucleotide-free Rac (GST–RacG15A) to isolate the active fraction of P-REX1. Then the supernatant, containing the inactive fraction of P-REX1, was subjected to immunoprecipitation

with anti-FLAG antibodies. Active and inactive P-REX1 fractions were then assayed by Western blotting with anti-phospho-PKA substrate antibodies.

Production and purification of recombinant P-REX1 and RIα proteins

RIα recombinant protein was produced in *Escherichia coli* BL21 strain and precipitated using cAMP-agarose. Resin was washed with saline buffer, and RIα was eluted with cGMP (40 mM). Then gel filtration was performed, and RIα fractions were collected, concentrated, and preserved at −20 °C by dialysis with 40% glycerol. Recombinant P-REX1 protein was produced in mammalian cell cultures. HEK293T cells were grown in five 10-cm Petri dishes, transfected with HA–HaloTag–P-REX1 construct with Turbofect. 48 h after transfection, cell lysates from 2×10^8 cells were incubated with HaloLink resin following the HaloTag Quick purification protocol (Promega). Purified proteins were quantified by the Bradford method. SDS-PAGE, Coomassie staining and Western blotting were performed to confirm protein integrity.

P-REX1 in vitro activation and interaction assays

To assess the direct interaction, *in vitro*, of P-REX1 with cAMP-bound RIα or type I PKA holoenzyme cAMP-agarose or (R_p)-8-AHA-cAMP were used for pulldown experiments. A mix of purified P-REX1 and RIα (0.5 and 1 μg, considering the RIα as a constitutive dimer) was prepared in lysis buffer containing 50 μM IBMX. The mix was incubated with 20 μl of cAMP-agarose or (R_p)-8-AHA-cAMP-agarose for 12 h at 4 °C. Samples were centrifuged at 5000 rpm for 2 min at 4 °C, and beads were washed three times with lysis buffer containing 1% Triton. To assess *in vitro* activation of P-REX1 by direct interaction with RIα, a mix of P-REX1 and RIα was prepared in lysis buffer containing 1% Triton and 10 mM $MgCl_2$. The mix was incubated with GST–RacG15A-Sepharose beads for 45 min in rocking agitator at 4 °C. Samples were centrifuged at 5000 rpm for 2 min at 4 °C, and beads were washed three times with lysis buffer. Finally (for both pulldowns), beads were resuspended in 1× Laemmli sample buffer containing mercaptoethanol, boiled for 5 min, and processed for SDS-PAGE and immunoblot.

Fluorescence microscopy

PAE cells were seeded at low density on gelatin-coated glass-bottom dishes. Cells were starved for 16 h with serum-free medium and stimulated with PGE_2 or butaprost (10 μM) for 15 min. Subsequently, cells were fixed in 4% paraformaldehyde in PBS for 20 min, washed twice with PBS, and prepared for conventional phalloidin and DAPI staining. Cell images were visualized in a Nikon Eclipse Ti inverted fluorescence microscope using a Plan Apo VC 1.4 oil immersion objective and captured with a Digital sight iXon Ultra ANDOR EMCCD camera. Images for F-actin and nuclear staining were obtained with Texas Red and UV filters, respectively, and analyzed with NIS-Elements Advanced Nikon software.

Wound-closure assay

PAE cells were seeded on 0.02% gelatin in 12-well plates. After 24 h, cells were starved with serum-free DMEM for 12 h. Mitomycin C was added (12 μM, Sigma, catalog no. M0440) after 10 h of starvation. Migration assays were initiated by wounding cell monolayers with a pipette tip. Cells were washed three times with PBS and stimulated with prostaglandin E_2 (1 μM), butaprost (10 μM), or 10% FBS in 2 ml of DMEM. After 24 h, cells were fixed with 4% paraformaldehyde, stained with crystal violet, washed with PBS, and photographed.

Chemotaxis assays

The effect of PGE_2 (1 μM), butaprost (10 μM), sphingosine 1-phosphate (1 μM) and hepatocyte growth factor (10 ng/ml) on PAE endothelial cells chemotaxis was assessed in Boyden chambers essentially as described previously (34). 48-Well chambers were used with gelatin-coated filters having 8-μm pores. Cells that were starved of serum for 14 h were washed with PBS, gently trypsinized, washed, and resuspended at 100,000 cells per 100 μl of serum free-DMEM. Chemotaxis assays were done with 50,000 cells per well leaving cells to migrate for 6 h at 37 °C. Then, cells were fixed with methanol and stained with crystal violet. Cells on the top side of the filter were removed with a cotton swab, and those at the bottom of the filter were observed under a ×20 objective to confirm the presence of stained cells. Densitometric analysis was performed with the ImageJ software.

Statistical analysis

Data are presented as means ± S.E. of at least 3–5 independent experiments. Densitometric quantitation of Western blottings and chemotaxis assays were done with ImageJ software. Active proteins, phosphorylated proteins, and interactions in pulldowns were normalized with total proteins and pulldown efficiency. Statistical analysis was performed using Sigma Plot 11.0, and graphs using Prism software version 6.0. Statistical test are indicated at the figure legends.

Author contributions—S. R. A.-G. and J. V.-P. conceptualization; S. R. A.-G., R. D. C.-V., G. R.-C., S. S. T., and J. V.-P. formal analysis; S. R. A.-G., R. D. C.-V., and L. B. O.-C. investigation; S. R. A.-G., J. C. d. R., and J. S. G. methodology; S. R. A.-G. writing-original draft; S. R. A.-G., J. S. G., S. S. T., and J. V.-P. writing-review and editing; R. D. C.-V. visualization; J. C. d. R., J. S. G., G. R.-C., S. S. T., and J. V.-P. supervision; J. S. G., G. R.-C., and S. S. T. resources; J. S. G., G. R.-C., S. S. T., and J. V.-P. funding acquisition; J. V.-P. project administration.

Acknowledgments—Technical assistance provided by Estanislao Escobar-Islas, Margarita Valadez, David Pérez, and Jaime Estrada Trejo is acknowledged.

References

1. Howe, A. K. (2004) Regulation of actin-based cell migration by cAMP/PKA. *Biochim. Biophys. Acta* **1692,** 159–174 CrossRef Medline
2. Taylor, S. S., Zhang, P., Steichen, J. M., Keshwani, M. M., and Kornev, A. P. (2013) PKA: lessons learned after twenty years. *Biochim. Biophys. Acta* **1834,** 1271–1278 CrossRef Medline
3. Knighton, D. R., Zheng, J. H., Ten Eyck, L. F., Ashford, V. A., Xuong, N. H., Taylor, S. S., and Sowadski, J. M. (1991) Crystal structure of the catalytic subunit of cyclic adenosine monophosphate-dependent protein kinase. *Science* **253,** 407–414 CrossRef Medline

4. Torres-Quesada, O., Mayrhofer, J. E., and Stefan, E. (2017) The many faces of compartmentalized PKA signalosomes. *Cell. Signal.* **37,** 1–11 CrossRef Medline
5. Lim, C. J., Han, J., Yousefi, N., Ma, Y., Amieux, P. S., McKnight, G. S., Taylor, S. S., and Ginsberg, M. H. (2007) α4 integrins are type I cAMP-dependent protein kinase-anchoring proteins. *Nat. Cell Biol.* **9,** 415–421 CrossRef Medline
6. Paulucci-Holthauzen, A. A., Vergara, L. A., Bellot, L. J., Canton, D., Scott, J. D., and O'Connor, K. L. (2009) Spatial distribution of protein kinase A activity during cell migration is mediated by A-kinase anchoring protein AKAP Lbc. *J. Biol. Chem.* **284,** 5956–5967 CrossRef Medline
7. Chávez-Vargas, L., Adame-García, S. R., Cervantes-Villagrana, R. D., Castillo-Kauil, A., Bruystens, J. G., Fukuhara, S., Taylor, S. S., Mochizuki, N., Reyes-Cruz, G., and Vázquez-Prado, J. (2016) Protein kinase A (PKA) type I interacts with P-Rex1, a Rac guanine nucleotide exchange factor: effect on PKA localization and P-Rex1 signaling. *J. Biol. Chem.* **291,** 6182–6199 CrossRef Medline
8. Kamiyama, M., Pozzi, A., Yang, L., DeBusk, L. M., Breyer, R. M., and Lin, P. C. (2006) EP2, a receptor for PGE2, regulates tumor angiogenesis through direct effects on endothelial cell motility and survival. *Oncogene* **25,** 7019–7028 CrossRef Medline
9. Yang, L., Gilbert, M. L., Zheng, R., and McKnight, G. S. (2014) Selective expression of a dominant-negative type Iα PKA regulatory subunit in striatal medium spiny neurons impairs gene expression and leads to reduced feeding and locomotor activity. *J. Neurosci.* **34,** 4896–4904 CrossRef Medline
10. Bos, J. L. (2006) Epac proteins: multi-purpose cAMP targets. *Trends Biochem. Sci.* **31,** 680–686 CrossRef Medline
11. Boshart, M., Weih, F., Nichols, M., and Schütz, G. (1991) The tissue-specific extinguisher locus TSE1 encodes a regulatory subunit of cAMP-dependent protein kinase. *Cell* **66,** 849–859 CrossRef Medline
12. Bachmann, V. A., Mayrhofer, J. E., Ilouz, R., Tschaikner, P., Raffeiner, P., Röck, R., Courcelles, M., Apelt, F., Lu, T. W., Baillie, G. S., Thibault, P., Aanstad, P., Stelzl, U., Taylor, S. S., and Stefan, E. (2016) Gpr161 anchoring of PKA consolidates GPCR and cAMP signaling. *Proc. Natl. Acad. Sci. U.S.A.* **113,** 7786–7791 CrossRef Medline
13. Welch, H. C., Coadwell, W. J., Ellson, C. D., Ferguson, G. J., Andrews, S. R., Erdjument-Bromage, H., Tempst, P., Hawkins, P. T., and Stephens, L. R. (2002) P-Rex1, a PtdIns(3,4,5)P3- and G$\beta\gamma$-regulated guanine-nucleotide exchange factor for Rac. *Cell* **108,** 809–821 CrossRef Medline
14. Welch, H. C. (2015) Regulation and function of P-Rex family Rac-GEFs. *Small GTPases* **6,** 49–70 CrossRef Medline
15. Vázquez-Prado, J., Bracho-Valdés, I., Cervantes-Villagrana, R. D., and Reyes-Cruz, G. (2016) G$\beta\gamma$ pathways in cell polarity and migration linked to oncogenic GPCR signaling: potential relevance in tumor microenvironment. *Mol. Pharmacol.* **90,** 573–586 CrossRef Medline
16. Cervantes-Villagrana, R. D., Adame-Garcia, S. R., Garcia-Jimenez, I., Color-Aparicio, V. M., Beltran-Navarro, Y. M., Konig, G. M., Kostenis, E., Reyes-Cruz, G., Gutkind, J. S., and Vazquez-Prado, J. (2018) G$\beta\gamma$ signaling to the chemotactic effector P-REX1 and mammalian cell migration is directly regulated by Gαq and Gα13 proteins. *J. Biol. Chem.* **294,** 531–546 CrossRef
17. Lucato, C. M., Halls, M. L., Ooms, L. M., Liu, H. J., Mitchell, C. A., Whisstock, J. C., and Ellisdon, A. M. (2015) The phosphatidylinositol (3,4,5)-trisphosphate-dependent Rac exchanger 1. Ras-related C3 botulinum toxin substrate 1 (P-Rex1·Rac1) complex reveals the basis of Rac1 activation in breast cancer cells. *J. Biol. Chem.* **290,** 20827–20840 CrossRef Medline
18. Hernández-Garcia, R., Iruela-Arispe, M. L., Reyes-Cruz, G., and Vázquez-Prado, J. (2015) Endothelial RhoGEFs: a systematic analysis of their expression profiles in VEGF-stimulated and tumor endothelial cells. *Vascul. Pharmacol.* **74,** 60–72 CrossRef Medline
19. Carretero-Ortega, J., Walsh, C. T., Hernández-García, R., Reyes-Cruz, G., Brown, J. H., and Vázquez-Prado, J. (2010) Phosphatidylinositol 3,4,5-triphosphate-dependent Rac exchanger 1 (P-Rex-1), a guanine nucleotide exchange factor for Rac, mediates angiogenic responses to stromal cell-derived factor-1/chemokine stromal cell derived factor-1 (SDF-1/CXCL-12) linked to Rac activation, endothelial cell migration, and *in vitro* angiogenesis. *Mol. Pharmacol.* **77,** 435–442 CrossRef Medline
20. Stefan, E., Malleshaiah, M. K., Breton, B., Ear, P. H., Bachmann, V., Beyermann, M., Bouvier, M., and Michnick, S. W. (2011) PKA regulatory subunits mediate synergy among conserved G-protein-coupled receptor cascades. *Nat. Commun.* **2,** 598 CrossRef Medline
21. Keshwani, M. M., Kanter, J. R., Ma, Y., Wilderman, A., Darshi, M., Insel, P. A., and Taylor, S. S. (2015) Mechanisms of cyclic AMP/protein kinase A- and glucocorticoid-mediated apoptosis using S49 lymphoma cells as a model system. *Proc. Natl. Acad. Sci. U.S.A.* **112,** 12681–12686 CrossRef Medline
22. Linglart, A., Menguy, C., Couvineau, A., Auzan, C., Gunes, Y., Cancel, M., Motte, E., Pinto, G., Chanson, P., Bougnères, P., Clauser, E., and Silve, C. (2011) Recurrent PRKAR1A mutation in acrodysostosis with hormone resistance. *N. Engl. J. Med.* **364,** 2218–2226 CrossRef Medline
23. Bruystens, J. G., Wu, J., Fortezzo, A., Del Rio, J., Nielsen, C., Blumenthal, D. K., Rock, R., Stefan, E., and Taylor, S. S. (2016) Structure of a PKA RIα recurrent acrodysostosis mutant explains defective cAMP-dependent activation. *J. Mol. Biol.* **428,** 4890–4904 CrossRef Medline
24. Smith, F. D., Langeberg, L. K., Cellurale, C., Pawson, T., Morrison, D. K., Davis, R. J., and Scott, J. D. (2010) AKAP-Lbc enhances cyclic AMP control of the ERK1/2 cascade. *Nat. Cell Biol.* **12,** 1242–1249 CrossRef Medline
25. Ledezma-Sánchez, B. A., García-Regalado, A., Guzmán-Hernández, M. L., and Vázquez-Prado, J. (2010) Sphingosine-1-phosphate receptor S1P1 is regulated by direct interactions with P-Rex1, a Rac guanine nucleotide exchange factor. *Biochem. Biophys. Res. Commun.* **391,** 1647–1652 CrossRef Medline
26. Kim, E. K., Yun, S. J., Ha, J. M., Kim, Y. W., Jin, I. H., Yun, J., Shin, H. K., Song, S. H., Kim, J. H., Lee, J. S., Kim, C. D., and Bae, S. S. (2011) Selective activation of Akt1 by mammalian target of rapamycin complex 2 regulates cancer cell migration, invasion, and metastasis. *Oncogene* **30,** 2954–2963 CrossRef Medline
27. Pan, D., Barber, M. A., Hornigold, K., Baker, M. J., Toth, J. M., Oxley, D., and Welch, H. C. (2016) Norbin stimulates the catalytic activity and plasma membrane localization of the guanine-nucleotide exchange factor P-Rex1. *J. Biol. Chem.* **291,** 6359–6375 CrossRef Medline
28. Hernández-Negrete, I., Carretero-Ortega, J., Rosenfeldt, H., Hernández-García, R., Calderón-Salinas, J. V., Reyes-Cruz, G., Gutkind, J. S., and Vázquez-Prado, J. (2007) P-Rex1 links mammalian target of rapamycin signaling to Rac activation and cell migration. *J. Biol. Chem.* **282,** 23708–23715 CrossRef Medline
29. Mavrakis, M., Lippincott-Schwartz, J., Stratakis, C. A., and Bossis, I. (2006) Depletion of type IA regulatory subunit (RIα) of protein kinase A (PKA) in mammalian cells and tissues activates mTOR and causes autophagic deficiency. *Hum. Mol. Genet.* **15,** 2962–2971 CrossRef Medline
30. Vigil, D., Blumenthal, D. K., Brown, S., Taylor, S. S., and Trewhella, J. (2004) Differential effects of substrate on type I and type II PKA holoenzyme dissociation. *Biochemistry* **43,** 5629–5636 CrossRef Medline
31. Barber, M. A., Hendrickx, A., Beullens, M., Ceulemans, H., Oxley, D., Thelen, S., Thelen, M., Bollen, M., and Welch, H. C. (2012) The guanine-nucleotide-exchange factor P-Rex1 is activated by protein phosphatase 1α. *Biochem. J.* **443,** 173–183 CrossRef Medline
32. Castellone, M. D., Teramoto, H., Williams, B. O., Druey, K. M., and Gutkind, J. S. (2005) Prostaglandin E2 promotes colon cancer cell growth through a Gs-axin-beta-catenin signaling axis. *Science* **310,** 1504–1510 CrossRef Medline
33. Guilluy, C., Dubash, A. D., and García-Mata, R. (2011) Analysis of RhoA and Rho GEF activity in whole cells and the cell nucleus. *Nat. Protoc.* **6,** 2050–2060 CrossRef Medline
34. Guzmán-Hernández, M. L., Vázquez-Macías, A., Carretero-Ortega, J., Hernández-García, R., García-Regalado, A., Hernández-Negrete, I., Reyes-Cruz, G., Gutkind, J. S., and Vázquez-Prado, J. (2009) Differential inhibitor of G$\beta\gamma$ signaling to AKT and ERK derived from phosducin-like protein: effect on sphingosine 1-phosphate-induced endothelial cell migration and in vitro angiogenesis. *J. Biol. Chem.* **284,** 18334–18346 CrossRef Medline